Characterization of the Cyclic Short-Time Variation of Indoor Power-line Channels Response

J.A. Cortés, F.J. Cañete, L. Díez and J.T. Entrambasaguas

Departamento de Ingeniería de Comunicaciones
E.T.S.I. de Telecomunicación, University of Málaga
Málaga, Spain

Abstract—**Indoor power-line channels response exhibits a time-varying behaviour with a twofold nature. The first one is the well-known long-term variation caused by the connection and disconnection of electrical devices. The second one is a short-time variation, synchronous to the mains, whose origin is the dependence of the impedance presented by electrical devices on the mains voltage [1]. The purpose of this paper is to assess the importance of this latter aspect in actual channels. To this end, a measurement procedure able to extract these short-time variations is described at first. Afterwards, a statistical analysis of the results obtained from a measurement campaign performed at different scenarios is given. Specifically, the delay spread, the peak excursion and the rate of change of the frequency response in the band from 1MHz to 20MHz are presented and discussed.**

Keywords- Time-varying channel, LPTV system, measurement system, delay spread, frequency response excursion, frequency response rate of change.

I.   INTRODUCTION

Traditionally, broadband measurements of indoor power-line channels response have been undertaken based on the assumption of an LTI (Linear Time-Invariant) channel model with several additive noise components [2,3]. In this context, changes in the response occur only as a result of the connection or disconnection of electrical appliances to the grid, leading to the well-known long-term time variations [4]. However, due to the dependence of the impedance presented by electrical devices on mains voltage [1], it also exhibits a short-time variation. Since this variation is also periodic, the channel response can be modeled by a linear periodically time-varying (LPTV) system [1]. This paper presents a characterization of the cyclic short-time behavior of the channel response.

Measurements presented up to now in the literature [2,3,4], which seem to corroborate LTI channel models, show no trace of these time variations because they have been carried out without using the mains time base as a reference. A measurement procedure and signal processing algorithms able to extract the cyclic properties of the channel frequency response are described in section II. Based on this methodology, a statistical analysis of measurement results performed at different scenarios in the band from 1MHz to 20MHz is presented. Statistics of parameters like the delay spread, the peak excursion and the rate of the change of the frequency response, given in section III, may be particularly helpful for the design of digital communication systems.

II.   MEASUREMENT METHODOLOGY

The measure of the channel frequency response has been done with the setup shown in fig. 1. The transmitter side is formed by a PC with a signal generation board (SGB) and a coupling circuit (CC), whose major purpose is to protect the board from the mains and to suppress spectrum replicas, i.e., to serve as a reconstruction filter. At the receiver side, a PC hosts a data acquisition board (DAB) used to capture the received signal at a rate of f_S samples/s. This board is also connected to the grid through a coupling circuit that attenuates the mains signal strong enough to protect the board but leaves a weak trace of it that allows its use as a time reference. Collected data are real-time transferred to the host PC to analyze them later, in differed time. This arrangement permits recording signal lengths of hundreds of mains cycles.

The sounding signal generated by the transmitter is composed of the sum of N harmonically related sinusoids. The frequency of these sinusoids is given by $f=k\Delta f$, with Δf =25·10^6/512≈48.83kHz, which corresponds to the transmission of N=512 sinusoids in the bandwidth from 0Hz to 25MHz. However, since the pass band of the coupling circuits extends from 1MHz to 20MHz, only sinusoids with indexes in the range $22 \leq k \leq 409$ are finally launched into the grid.

The signal acquired by the DAB, $y(n)$, has a length equivalent to C times the mains period, T_0 (20ms in Europe). Each cycle c is divided in L regular intervals of duration $T_\ell = T_0 / L$. The amplitude and phase of the received sinusoids in the ℓ-th interval of the c-th cycle is estimated by calculating the *2N*-point DFT (Discrete Fourier Transform) of the signal

$$y_\ell^c(n) = y(2NLc + 2N\ell + n) \qquad (1)$$

with $0 \leq n \leq 2N - 1$, leading to

$$Y^c(\ell,k) = \frac{1}{2N} \sum_{n=0}^{2N-1} y_\ell^c(n) \cdot e^{-j\frac{2\pi}{2N}kn} \qquad (2)$$

Provided that the channel remains effectively invariant during the time that the impulse response lasts, the so-called slow-variation assumption applies and it is possible to select a value for T_ℓ so that $Y^c(\ell,k)$ can be also expressed as [1],

$$Y^c(\ell,k) = H(\ell,k) \cdot X(k) + N^c(\ell,k) \qquad (3)$$

where $X(k)$ is the Fourier series coefficient of the sinusoid transmitted at frequency $f=k\Delta f$, $H(\ell,k)$ is the sampled version
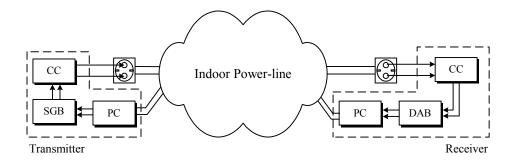
Figure 1. Frequency response measurement setup

of the channel frequency response, $H(t,f)|_{t=\ell T_\ell, f=k\Delta f}$, and $N^c(\ell,k)$ is the instantaneous power spectral density (PSD) of the noise received during the ℓ-th interval of the c-th cycle.

An estimate of $H(\ell,k)$ has been obtained by means of a synchronized averaging of the values in (3)

$$\hat{H}(\ell,k) = \frac{1}{X(k)} \frac{1}{C} \sum_{c=0}^{C-1} Y^c(\ell,k) \qquad (4)$$

with C fixed to 234 and L to 976, what has lead to a T_ℓ value of approximately 20.5μs.

Since the averaging in (4) is performed over hundreds of cycles, the effect of the accumulated jitter (also known as long-term-jitter) of the mains can not be neglected. This jitter has been calculated from the zero-crossings of the weak trace of the mains left by the coupling circuit.

The aforementioned measurement methodology lies in two major assumptions. The first one is that the channel is substantially invariant during T_ℓ, and the second is that the channel behaves as a linear system for the communication signal. In order to corroborate both premises, the transmitted signal and the received algorithms have been modified to implement a DMT (Discrete Multitone) system [5]. The number of carriers has been fixed to 512, and the cyclic prefix length has been varied to obtain symbol lengths (T_{DMT}) in the range from 21.48μs to 27.5μs. This procedure allows the estimation of the frequency response at $T_0/T_{DMT} < L$ time instants over a period, which is, in fact, an undersampled version of the one obtained with the sinusoids. Since no significant changes have been found between the estimates performed with both methods, it can be concluded that both premises are verified.

III.   STATISTICAL ANALYSIS OF THE CHANNEL RESPONSE

The measurement methodology described in section II has been employed to register more than fifty actual channels in three different scenarios: a university building (laboratories and offices), an apartment of about 80m^2 and a detached house with, approximately, 300m^2. Channels were established between randomly selected outlets with no special care about the devices connected in their neighborhood.

Representative examples of the time variations measured in the frequency responses are given in [1]. However, in order to asses the real importance of these short-time changes, a statistical analysis is now presented. Concretely, three parameters are studied: the peak excursion and rate of change of the frequency response and the delay spread.

A. Peak excursion and rate of change of the frequency response

Changes in the frequency response affect not only to its module but to its phase as well. This circumstance is clearly shown in fig. 2, where the evolution of the frequency response in a cycle is depicted in the complex plane. It is frequent to find situations like the one in fig.2 (b), in which the attenuation remains nearly constant while the phase experiences fluctuations of up to π rad. In other occasions, both the module and phase vary, as in fig. 2 (a).
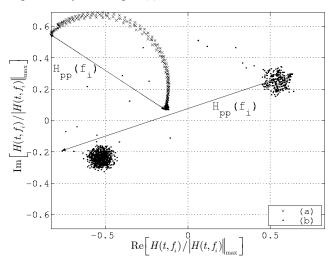

Figure 2. Normalized real and imaginary part of the frequency response of two channels in a 20ms time interval. (a) Apartment at f$_i$=2.64MHz and (b) university laboratory at f$_i$=12.5MHz

To reflect the maximum magnitude of both, amplitude and phase variations, the peak excursion of the frequency response is defined according to

$$H_{pp}(f) = \max_{t_1,t_2}\left\{\left|H(t_1,f) - H(t_2,f)\right|\right\} \qquad (5)$$

327

with $t_1, t_2 \in [0, T_0)$. The peak excursion has the clear geometrical interpretation shown in fig. 2: the maximum distance between values taken by the frequency response in a cycle. However, in order to compare peak excursions calculated in different frequencies and channels, it is better to express (5) relative to the time-averaged (over a cycle) frequency response amplitude

$$\widetilde{H}_{pp}(f) = \frac{H_{pp}(f)}{<|H(t,f)|>} \tag{6}$$

The values of $\widetilde{H}_{pp}(f)$ have been computed for all the frequencies of the whole set of measured channels with the only exception of those corresponding to notches of the frequency response, in which the estimation of $H(t,f)$ is not reliable. Afterwards, the calculated values have been grouped in subsets according to the scenario (university, apartment or detached house) in which the corresponding frequency response was measured. The cumulative distribution functions (cdf) associated to each subset and to the overall set of frequencies and channels are drawn in fig. 3.
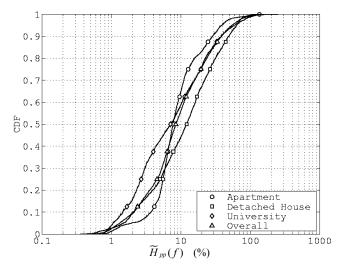

Figure 3.   Cdf of the relative peak excursion of the frequency response expressed as a percentage

As can be observed, significant excursions occur in all the scenarios, with changes greater than 10% in approximately 40% of the analyzed frequencies. It is worth noting that the function depicted in fig. 3 tries to indicate the probability of finding a certain value of $\widetilde{H}_{pp}(f)$ when the response of an arbitrary channel is observed at a randomly selected frequency. However, this does not mean that the channel behaves homogeneously in all the analyzed band. In fact, time variations are generally frequency selective, i.e. they affect only a portion of the whole band. This end can be observed by computing the rms value of the relative peak excursions measured in each channel. Thus, denoting by $\overline{(\cdot)}$ the ensemble average over the samples of the considered channel, the rms value of $\widetilde{H}_{pp}(f)$ can be calculated as

$$H_{pp}rms = \left[\overline{\left(\widetilde{H}_{pp}(f) - \overline{\widetilde{H}_{pp}(f)} \right)^2} \right]^{1/2} \tag{7}$$

Figure 4 depicts the values of (7) expressed as a percentage relative to the averaged value of the peak excursion, $\overline{\widetilde{H}_{pp}(f)}$. As shown, relative values of the rms peak excursion, denoted by $\widetilde{H}_{pp}rms$, may be even greater than 75% in 50% of the analyzed channels, what highlights the remarkable frequency selective character of the time variations.
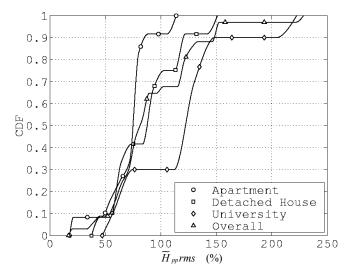

Figure 4.   Cdf of the relative rms value of the peak excursion in each channel expressed as a percentage

With the aim of quantifying the velocity of the changes in the frequency response, the relative rate of change of $H(t,f)$ is defined as

$$\widetilde{\Delta H}(f) = \max_t \left\{ \frac{|H(t+T_\ell,f) - H(t,f)|}{|H(t,f)|} \right\} \tag{8}$$

with $t \in [0, T_0)$.

Following a similar procedure to the one employed with $\widetilde{H}_{pp}(f)$, the values of $\widetilde{\Delta H}(f)$ computed for the frequencies of all the measured channels have been grouped according to their corresponding scenario. Fig. 5 shows the cdf estimated for each subset and the one for the overall set of frequencies and channels.

The rate at which changes occur in the frequency response is clearly highlighted in these curves, in which 40% of the analyzed frequencies show relative variations of up to between 2% and 6% (depending on the scenario) in just a time interval T_ℓ (20.5μs). It is also interesting to note that the environments with the highest rates of change in the frequency response also suffer the highest peak excursions (see fig. 3).

Results presented in this subsection may be particularly interesting for the design of the equalization stage of any digital communication system.
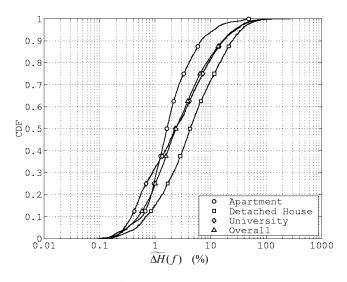
328

Figure 5. Cdf of the the relative rate of change of the frequency response expressed as a percentage

Figure 6. Cdf of the delay spread

Nevertheless, when focusing on a DMT system, which is considered by now the most adequate technique for such frequency-shaped channels, the values of $\widetilde{H}_{pp}(f)$ and $\widetilde{\Delta H}(f)$ are helpful magnitudes to determine the dynamic range and rate of adaptation needed for the taps of the frequency equalizer (FEQ) usually employed in these systems.

B. Delay spread

The delay spread is a parameter typically used for wide-band characterization of frequency selective channels and has plain application to the design of digital communication systems. It measures the temporal dispersion of the channel or, equivalently, the effective length of its impulse response. In power-line channels, due to the periodic variation of the impulse response, the delay spread will be also periodical.

Denoting by $h(t, t - \tau)$ the response of the channel at time t to an impulse applied at time $t - \tau$, the power delay profile (also called delay power spectrum [6,7]) of the channel can be computed as

$$P(t, \tau) = |h(t, t - \tau)|^2 \tag{9}$$

The mean excess delay is then defined as

$$d(t) = \frac{\int_0^\infty \tau \cdot P(t, \tau) \cdot d\tau}{\int_0^\infty P(t, \tau) \cdot d\tau} \tag{10}$$

and the delay spread as

$$\sigma(t) = \sqrt{\frac{\int_0^\infty (\tau - d(t))^2 \cdot P(t, \tau) \cdot d\tau}{\int_0^\infty P(t, \tau) \cdot d\tau}} \tag{11}$$

For each measured channel, $\sigma(t)$ has been computed for L time instants along a cycle and grouped in a subset according to their corresponding scenario. The cdf associated to each environment is depicted in fig. 6.
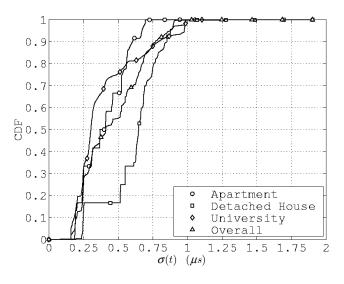
As seen, mean values of the delay spread are in the range from 0.3µs to 0.65µs. Similarly, it can be observed that the channels measured in the detached house experience the greatest delay spreads. Considering that the power grid of the detached house was the larger one and had the more branched topology, these results reveal a clear correspondence between the dispersion of the channel and its physical layout. Hence, the more branched the network is, the higher number of reflections the signal will found in its way between the transmitter and the receiver, and the stronger time dispersion it will suffer.

The time-averaged delay spread of each channel, σ, can be calculated as

$$\sigma \equiv \langle \sigma(t) \rangle = \frac{1}{T_0} \int_0^{T_0} \sigma(t) dt \tag{12}$$

It is interesting to study the relation between this parameter and the average coherence bandwidth of the channel [6,7], a figure that indicates the range of frequencies in which the frequency response presents strong correlation values. The coherence bandwidth, $B_C(t)$, at time t is more precisely defined as the frequency separation for which the spaced-frequency correlation function, given by [7]

$$R(t, \Delta f) = \int_{-\infty}^{-\infty} H(t, f) H^*(t, f + \Delta f) df \tag{13}$$

falls down a given threshold, usually 0.9.

The time-averaged coherence bandwidth (at 0.9), B_C, is then calculated as

$$B_C \equiv \langle B_C(t) \rangle = \frac{1}{T_0} \int_0^{T_0} B_C(t) dt \tag{14}$$

Fig. 7 depicts a clear relation between the values of σ and B_C estimated in the overall set of measured channels, which can be approximated by

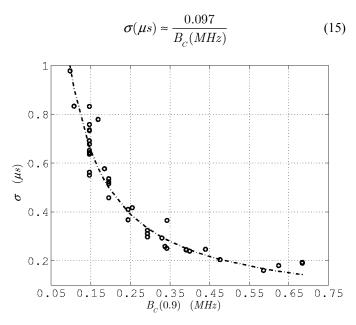$$\sigma(\mu s) \approx \frac{0.097}{B_C(MHz)} \qquad (15)$$

Figure 7.   Mean delay spread versus coherence bandwidth at 0.9

The time-averaged delay spread is useful as a reference to calculate the rms value of the delay spreads measured in each channel,

$$\sigma_{rms} = \sqrt{\langle [\sigma(t) - \langle \sigma(t) \rangle]^2 \rangle} \qquad (16)$$

The cdf of the values in (16) are depicted in fig. 8. For the sake of clarity, the values of σ_{rms} have been expressed as a percentage relative to $\langle \sigma(t) \rangle$ and denoted by $\tilde{\sigma}_{rms}$.
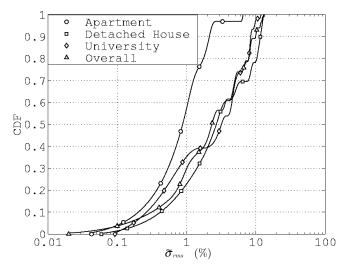

Figure 8.   Cdf of the relative rms delay spread expressed as a percentage

Considering the overall set of measured channels, it can be seen that 80% of them experience relative variations smaller than 8%. This result discloses that the effective length of the impulse response does not suffer significant variations along its period. This fact, although somewhat surprising at the sight of fig. 3 and, specially, fig. 5, is the normal situation in other time varying channels like mobile radio ones.

Again, implications derived from the curves in fig. 8 may be of considerable interest for the design of a DMT system. In particular, for the cyclic prefix length, whose value is strongly dependent on the dispersion of the channel [5]. These results indicate that cyclic prefix length can be chosen without taken special care about the time instant in which the delay spread of the channel is estimated.

IV.   CONCLUSIONS

This paper has presented a characterization of the short-time variations of indoor power-line channels response in the frequency band from 1MHz to 20MHz. A measurement methodology capable of extracting these time variations has been firstly described. Afterwards, a statistical analysis of the results obtained in a measurement campaign performed at three different scenarios has been given.

It has been shown that, on average, the frequency response experiences peak excursions greater than 10% in approximately 40% of the analyzed frequencies. Moreover, relative changes in the frequency response of up to between 2% and 6% occur in a time interval of just 20.5µs in 40% of the cases. It has been also revealed that this time variations have a very frequency selective character.

Despite of the remarkable frequency response variations, the study of the delay spread has evidenced that the effective length of the impulse response does not suffer significant variations, similarly to the case of mobile radio channels. The relation between the time-averaged delay spread and coherence bandwidth in power-line channels has been stated.

REFERENCES

[1]   F.J. Cañete, J.A. Cortés, L. Díez, J.T. Entrambasaguas and J.L. Carmona, "Fundamentals of the Cyclic Short-Time Variation of Indoor Power-line Channels," *in Proc. International Symposium on Power-Line Communications and its Applications (ISPLC)*, 2005, Vancouver, Canada.

[2]   H. Philipps, "Performance measurements of power line channels at high frequencies," *in Proc. International Symposium on Power-Line Communications and its Applications (ISPLCA)*, 1998, pp. 229–237.

[3]   D. Liu, E. Flint, B. Gaucher, and Y. Kwark, "Wide band AC power line characterization," *IEEE Trans. on Consumer Electronics*, vol. 45, issue 4, pp. 1087–1097, Nov 1999.

[4]   F. Cañete, L. Díez, J. Cortés, and J. Entrambasaguas, "Broadband modelling of indoor power-line channels," *IEEE Trans. on Consumer Electronics*, vol. 48, issue 1, pp. 175–183, Feb 2002

[5]   Edfors, O.; Sandell, M.; Van de Beek, J.J.; Landström, D.; Sjöber, F. , "An introduction to orthogonal-frequency division multiplexing," Research Report 1996:16, Division of Signal Processing, Luleå University of Technology, Sep. 1996.

[6]   B. Sklar, "Rayleigh Fading Channels in Mobile Digital Communications Systems Part I: Characterization", *IEEE Comm. Mag.*, vol. 35, Issue 7, pp. 90-100, July 1997.

[7]   J.G. Proakis, "Digital Communications", McGraw-Hill, 1995.